Size dependent reaction kinetics of small gold clusters with carbon monoxide: Influence of internal degrees of freedom and carbonyl complex stability

J. Hagen[1], L.D. Socaciu[1], U. Heiz[2], T.M. Bernhardt[1,a], and L. Wöste[1]

[1] Institut für Experimentalphysik, Freie Universität Berlin, Arnimallee 14, 14195 Berlin, Germany
[2] Abteilung für Oberflächenchemie und Katalyse, Universität Ulm, 89069 Ulm, Germany

Abstract. The reactions of free gold clusters Au^-, Au_2^-, and Au_3^- with carbon monoxide are studied in an rf-octopole ion trap experiment at cryogenic temperatures. While Au^- is unreactive toward CO over the whole temperature range investigated, the two and three atom cluster anions show a maximum adsorption of two CO molecules at temperatures below 250 K. From time resolved trapping experiments the strongly cluster size dependent reaction kinetics are obtained and a distinct reaction mechanism is deduced. The size dependence of the measured rate coefficients reveals the preferred formation and particular stability of the carbonyl complex $Au_3(CO)_2^-$. Through RRK analysis of the absolute termolecular rate coefficients we are able to estimate the binding energy of CO to Au_2^- and Au_3^-.

1 Introduction

The remarkable size and charge state dependence of the reactivity of free gold clusters toward small molecules was first recognized more than a decade ago [1]. The close relation of gold cluster electron affinity and reactivity toward molecular oxygen, *e.g.*, has been demonstrated by several groups [1–4]. The reaction of gold cluster ions with carbon monoxide has also been reported and an enhanced stability of several particular carbonyls was observed [5,6]. CO binding to free clusters with less than four atoms, however, is known to be rather weak [3,7,8] and Au_{1-3}^- carbonyls could even not be detected in some experiments [6]. We recently reported on the low temperature synthesis and catalytic activity of free carbonyls of the negatively charged gold dimer and trimer in a radio frequency(rf)-ion trap experiment [4,9]. In the present contribution we now aim to reveal the formation mechanism of the mono- and dicarbonyl complexes of these small gold cluster anions. As gold nano-particles and clusters currently attract considerable interest for their low temperature catalyic activity in a variety of reactions including CO combustion [10], the reaction mechanism of small gold clusters with CO is of particular importance to add to the understanding of the catalytic properties of these nano-scale gold materials.

2 Experiment

To study the mechanism of Au_n^- cluster reactions, a variable temperature rf-octopole ion trap inserted into a tandem quadrupole mass spectrometer is employed. In comparison to flow tube reactor experiments, the use of an rf-ion trap to investigate gas phase metal cluster reactions has the advantage that the experimental conditions, *i.e.*, reaction temperature, reactant partial pressures, total pressure, and reaction time, can be precisely determined. The general experimental setup is described in detail elsewhere [11] and will only be outlined briefly here. The gold cluster anions are produced by an ion sputtering source. Mass selection is achieved *via* a first quadrupole mass filter. The mass-selected cluster ion beam then enters the octopole ion trap, which is filled up to space charge limit with metal cluster ions (about 10^4 clusters per mm^3). The trap is prefilled with a helium partial pressure on the order of 1 Pa and the clusters are thermalized to the temperature of the background helium gas in the trap within few milliseconds. A closed cycle helium cryostat attached to the trap allows temperature adjustment in the range
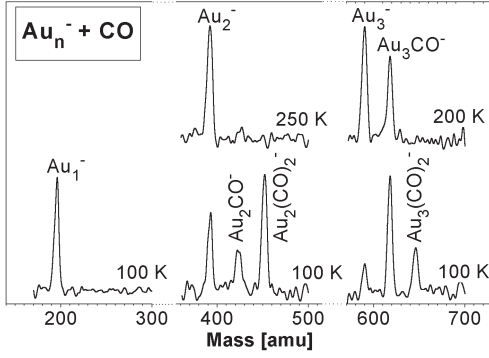
ᵃ e-mail: tbernhar@physik.fu-berlin.de

Fig. 1. Product ion distributions analyzed after trapping Au^-, Au_2^-, and Au_3^-, respectively, inside the octopole trap filled with 1 Pa of helium and a small partial pressure of carbon monoxide. Reaction temperatures are as indicated. Note that no other reaction products are observed even after 10 s trapping period.

Fig. 2. Kinetic traces of the reaction of Au_2^- (left) and Au_3^- (right) with CO at a reaction temperature of 100 K. The open symbols represent the normalized experimental data. The solid lines are obtained by fitting the integrated rate equations of the reaction mechanism (Eqs. (1, 2)) to the experimental data. In the case of the Au_2^- reaction the helium pressure in the trap is $p(He) = 0.96$ Pa and the carbon monoxide partial pressure amounts to $p(CO) = 0.24$ Pa. For the Au_3^- reaction $p(He) = 1.08$ Pa and $p(CO) = 0.02$ Pa.

between 20 and 350 K. Time-resolved kinetic measurements on the time scale of seconds are performed with small, well defined partial pressures of the reactant carbon monoxide present in the trap. For this purpose all ions are extracted from the trap after defined storage time by means of a pulsed electrostatic field and are subsequently mass-analyzed by a second quadrupole mass filter.

3 Results

No reaction products of Au^-, Au_2^-, and Au_3^- with carbon monoxide are detected at room temperature, even for storage times up to 10 seconds. This is in agreement with an earlier report [6]. In our experiment cooling of the rf-ion trap to temperatures below 250 K turned out to be necessary to detect reaction products between the gold cluster anions and carbon monoxide. In Figure 1 the product ion mass spectra of Au_{1-3}^- with CO in the ion trap are shown. The atom negative ion Au^- shows no reaction products at all temperatures investigated. However, cooling down leads in the case of Au_2^- and Au_3^- first to the formation of the mono-carbonyls and at the lowest temperatures to a maximum adsorption of two CO molecules as can be seen from the lower traces in Figure 1.

In order to deduce the reaction mechanism of the observed reactions, we record the reactant and product ion concentrations as a function of reaction time, *i.e.*, the residence time of the ions inside the trap. The resulting kinetic traces for Au_2^- as well as for Au_3^- at 100 K reaction temperature are depicted in Figure 2. The single points represent the experimental data normalized to the total ion concentration in the trap during reaction. The kinetic traces of Au_2^- and Au_3^- have a strikingly different appearance. This is even more pronounced considering that the reactive gas concentration in the ion trap in Figure 2b (Au_3^-) is less than one tenth of the CO concentration in Figure 2a (Au_2^-). In both cases, the Au_n^- signal decreases exponentially, but the carbonyl product concentrations show very different evolution as function of reaction time.
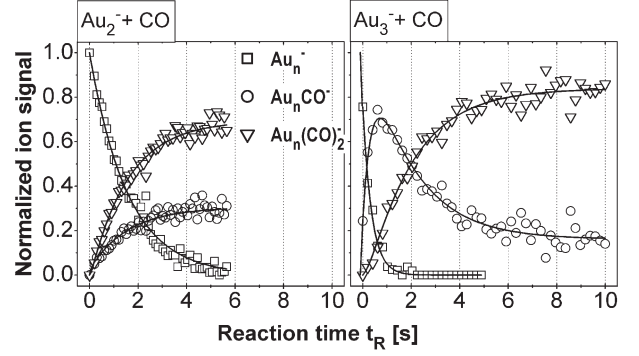
In the case of Au_3^- the monocarbonyl can clearly be identified as an intermediate with decreasing concentration at longer reaction times, whereas for Au_2^- the mono- and dicarbonyl concentrations rise simultaneously to reach an equilibrium.

The reaction mechanism for the observed kinetics is obtained by fitting the integrated rate equations of a proposed mechanism to the experimental data [12]. This procedure is very sensitive to the type of mechanism and we were able to rule out all but one possible mechanism. Most interestingly, the kinetics of both, Au_2^- as well as Au_3^-, are best fit by the same mechanism represented by the following equations:

$$Au_n^- + CO \rightarrow Au_nCO^- \qquad k_1 \qquad (1)$$
$$Au_nCO^- + CO \rightleftharpoons Au_n(CO)_2^- \qquad k_2, \ k_{-2} \qquad (2)$$
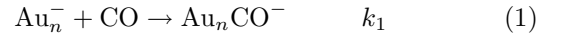
k_1, k_2, and k_{-2} are the rate coefficients for the different reaction steps. The adsorption of CO occurs sequentially with Au_nCO^- as an intermediate product. Purely consecutive reaction steps do not fit the experimental data and it is therefore essential to introduce a final equilibrium (Eq. (2)). The fits to the data are represented by the solid lines in Figure 2 and are an excellent match to the experimental results. The corresponding rate coefficients are listed in Table 1. Note that the fitting procedure results in pseudo first order rate coefficients $k^{(1)}$. The absolute three-body termolecular rate coefficients $k^{(3)}$ can be obtained eventually by division of $k^{(1)}$ with the concentration of the reactant CO and of the He buffer gas. $k^{(3)}$ values are listed in Table 1 for the adsorption reactions of the first CO.

4 Discussion

The following discussion aims to elucidate the origin of two striking results presented in the preceding section,

Table 1. Rate coefficients according to equations (1, 2) for Au_n^-.

n	$k_1^{(3)}$	$k_2^{(1)}$	$k_{-2}^{(1)}$	$K =$
	$[10^{-29}\ cm^6\ s^{-1}]$	$[s^{-1}]$	$[s^{-1}]$	$k_2^{(1)}/k_{-2}^{(1)}$
2	0.52 ± 0.03	13.2 ± 1.0	5.8 ± 0.8	2.3
3	23 ± 6	0.45 ± 0.12	0.087 ± 0.023	5.2

namely: (i) the fact that the measured rate coefficient for the reaction of the first CO with a gold cluster anion $k_1^{(3)}$ is more than 44 times larger for the trimer than for the dimer cluster anion (Tab. 1); and (ii) the qualitatively different appearance of the measured kinetic traces for the dimer and the trimer cluster ions (Fig. 2). For this purpose we will relate these observations to the number of internal degrees of freedom and the number of valence electrons of the gold carbonyl complexes.

Concerning the first result: Castleman and coworkers pointed out the important relation between the product formation rate and the possibility of intracluster energy redistribution, which is reflected by the number of internal vibrational degrees of freedom, for gas phase metal cluster reactions [13]. In the case of positively charged copper clusters this group observed a minimum number of seven atoms necessary for the cluster to form its own heat bath and thus to be able to accommodate the excess energy released during CO adsorption. Above seven atoms per cluster the reaction rate coefficients as a function of the number of atoms per cluster did not change significantly. However, this function showed the most dramatic increase going from the dimer to the trimer cluster. This might be rationalized considering that the dimer has only one internal coordinate, whereas for the trimer, the cluster potential energy surface becomes at least three dimensional which is a drastic change in terms of the possibility of internal energy redistribution. Hence the pronounced increase of the reaction rate going from the dimer to the trimer ion is expected to be intimately related to the rising number of internal degrees of freedom.

In order to further quantify this conclusion, we will treat the adsorption of the first CO (Eq. (1)) according to the Lindemann energy transfer model for association reactions which is represented by the following equations [14]:

$$Au_n^- + CO \rightleftharpoons Au_nCO^{-*} \qquad k_a,\ k_d \qquad (3)$$

$$Au_nCO^{-*} + He \rightarrow Au_n(CO)^- + He^* \qquad k_s \qquad (4)$$
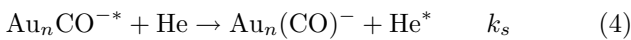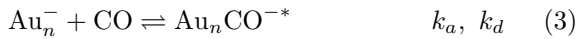
k_a is the association rate coefficient for the formation of the intermediate, energetically excited ion-molecule complex Au_nCO^{-*}, which can decompose *via* unimolecular decay back to the reactants with the rate coefficient k_d, if no stabilizing collision with a background helium atom takes place (rate coefficient k_s). Assuming all reaction steps to be of pseudo first order and employing steady state assumption for the intermediate, the overall third order rate expression is obtained to be [6]

$$k^{(3)} = \frac{k_a k_s}{k_d} \qquad (5)$$

in the kinetic low pressure regime, where $k_d \gg k_s[He]$. The association rate coefficient k_a as well as final stabilization rate coefficient k_s are well represented by ion-molecule collision rate coefficients according to Langevin theory and are cluster size independent [13]. The cluster size dependence of $k^{(3)}$ is thus contained in the unimolecular decomposition rate coefficient k_d of the metastable intermediate complex. In order to estimate k_d, we employ statistical Rice-Ramsperger-Kassel(RRK)-Theory. The RRK decomposition rate coefficient is [14]

$$k_d = \nu \left(\frac{E - E_0}{E} \right)^{S-1} \qquad (6)$$

for the given case that the total internal energy E, contained in S independent oscillators, is larger than the CO binding energy to the gold cluster E_0. ν is the frequency factor [15]. The internal energy E of the carbonyl complex is the sum of the potential energy gained in forming the complex E_0, the vibrational energy of the reactants, which is $E_{vib}(Au_n^-)$ before the reaction, because the CO molecules can be considered vibrationally cold at our reaction temperature, and finally the energy E_{free} in the translational and rotational degrees of freedom converted into internal energy of Au_nCO^{-*} [15]. The structure of the trimer anion is known to be linear [16] and thus $E_{vib}(Au_{2,3}^-) = (3n - 5)k_BT$ and $E_{free} = 2k_BT$ [15], with k_B being the Boltzmann constant and T the reaction temperature. This leads to

$$E = E_0 + E_{vib}(Au_n^-) + E_{free} = E_0 + (3n - 3)k_BT. \quad (7)$$

Assuming a non-linear geometry for the carbonyl complex with $S = 3N - 6$, where N is number of atoms in the monocarbonyl complex, results in the following unimolecular RRK decomposition rates for the two cluster sizes:

$$k_d(Au_2^-) = \nu \left(\frac{3k_BT}{E_0 + 3k_BT} \right)^5 \qquad (8)$$

$$k_d(Au_3^-) = \nu \left(\frac{6k_BT}{E_0 + 6k_BT} \right)^8. \qquad (9)$$

If now the assumption is made that the CO binding energies to Au_2^- and Au_3^- are similar, which is very reasonable according to recent theoretical work [17,18], we can calculate the ratio of the termolecular rate coefficients to be

$$\frac{k^{(3)}(Au_3^-)}{k^{(3)}(Au_2^-)} = \frac{k_d(Au_2^-)}{k_d(Au_3^-)} = \frac{(E_0 + 6k_BT)^8}{2^8(3k_BT)^3(E_0 + 3k_BT)^5}. \qquad (10)$$

Taking finally the experimental reaction temperature of $T = 100$ K and the measured rate coefficient ratio of 44, the CO binding energy E_0 on the small gold clusters can be obtained: $E_0 = 0.5$ eV. Note that this estimated value represents a mean value between the assumed similar CO binding energies to Au_2^- and Au_3^-. Comparison of this energy to known experimental as well as theoretical values reveals a very good agreement. Since the optimal CO bonding occurs for elements with partially occupied

d shell, CO is known to bind only weakly to coinage metals. The binding energy of CO to Au_2^- was determined in a different experiment to be 0.91 eV [8]. Theoretical calculations give in this case the values 0.77 eV [8] and 0.96 eV [19]. A recent theoretical work obtains 0.78 eV for the adsorption of CO onto Au_2^- and 0.76 eV onto Au_3^- [18].

This good agreement supports the outstanding influence of the increasing number of degrees of freedom, on which the RRK model is exclusively based, on the rate coefficients. Hence, the factor of 44 higher rate coefficient for the trimer reaction with CO can be largely ascribed to the considerably more efficient internal energy redistribution after initial CO adsorption in Au_3^- than in Au_2^-. This pronounced dependence of the internal vibrational energy redistribution (IVR) on cluster size, in particular when going from the dimer to the trimer was also noted in femtosecond laser experiments probing the cluster geometrical rearrangement after electron detachment in real time: counterintuitively, no oscillating wave packet motion is observed in the vibrational modes of the noble metal trimers, instead the energy is partitioned and dissipated within picoseconds between available degrees of freedom [20].

We will now discuss the second remarkable observation that both kinetic traces for Au_2^- and Au_3^-, respectively, although appearing clearly dissimilar (Fig. 2), can be described by the same underlying reaction mechanism (Eqs. (1, 2)). Analysis of Table 1 shows that the dissimilarity is due to the different ratio of the adsorption (k_2) and desorption (k_{-2}) rate coefficient of the second CO molecule for Au_2^- and Au_3^-. $K = k_2/k_{-2}$ is the equilibrium constant of the reaction in equation (2). K is larger than one for both cluster sizes, but the equilibrium is located by a factor of 2.3 more on the side of the final product $Au_3(CO)_2^-$ than on $Au_2(CO)_2^-$ (cf. Tab. 1). This points toward a significantly higher stability of $Au_3(CO)_2^-$ compared to all the other investigated carbonyl compounds. To explain the enhanced stability of certain free gold carbonyls, a simple electron counting scheme was suggested by other groups [5,6], considering Au s-valence electrons and two electrons donated per CO molecule. This leads to stable complexes for electron counts of, e.g., 8 (Au_7CO^+ [5], Au_5CO^- [6]) or 20 ($Au_{19}CO^+$ [5], $Au_{15}(CO)_2^-$ [6]). In this picture $Au_3(CO)_2^-$ would correspond to a stable 8 electron complex. However, recent theoretical investigations emphasize the importance of s-d hybridization due to relativistic effects in gold clusters [21]. Hence, the role of the d-electrons on the bonding in gold carbonyl complexes must not be neglected and an s-electron based delocalized shell type explanation of the complex stability is not justified according to [21]. The elucidation of the origin of the observed stability of $Au_3(CO)_2^-$ will therefore rely on future detailed *ab initio* calculations.

In conclusion, we presented for the first time cluster size dependent kinetic measurements conducted under well defined experimental conditions that lead to an unambiguous reaction mechanism and absolute rate coefficients. The size effects on the reaction rates are related to the number of internal degrees of freedom available for energy accommodation in the process of CO adsorption reaction. Furthermore, the enhanced stability of the complex $Au_3(CO)_2^-$ is suggested by a particular high equilibrium constant in favor of adsorption of the second CO molecule.

References

1. D.M. Cox, R. Brickman, K. Creegan, A. Kaldor, Z. Phys. D **19**, 353 (1991)
2. B.E. Salisbury, W.T. Wallace, R.L. Whetten, Chem. Phys. **262**, 131 (2000)
3. T.H. Lee, K.M. Ervin, J. Phys. Chem. **98**, 10023 (1994)
4. J. Hagen, L.D. Socaciu, M. Elijazyfer, U. Heiz, T.M. Bernhardt, L. Wöste, Phys. Chem. Chem. Phys. **4**, 1707 (2002)
5. M.A. Nygren, P.E.M. Siegahn, C. Jin, T. Guo, R.E. Smalley, J. Chem. Phys. **95**, 6181 (1991)
6. W.T. Wallace, R.L. Whetten, J. Phys. Chem. B **104**, 10964 (2000)
7. L. Lian, P.A. Hackett, D.M. Rayner, J. Chem. Phys. **99**, 2583 (1993)
8. G. Lüttgens, N. Pontius, P.S. Bechthold, M. Neeb, W. Eberhardt, Phys. Rev. Lett. **88**, 076102 (2002)
9. L.D. Socaciu, J. Hagen, T.M. Bernhardt, L. Wöste, U. Heiz, H. Häkkinen, U. Landman, J. Am. Chem. Soc. (submitted)
10. M. Haruta, Appl. Catal. A **222**, 427 (2001); A. Sanchez, S. Abbet, U. Heiz, W.-D. Schneider, H. Häkkinen, R.N. Barnett, U. Landman, J. Phys. Chem. A **103**, 9573 (1999); H. Häkkinen, S. Abbet, A. Sanchez, U. Heiz, U. Landman, Angew. Chem. **115**, 1335 (2003); Angew. Chem. Int. Ed. **42**, 1300 (2003)
11. L.D. Socaciu, J. Hagen, U. Heiz, T.M. Bernhardt, T. Leisner, L. Wöste, Chem. Phys. Lett. **340**, 282 (2001)
12. E. Schumacher, *DETMECH - Chemical Reaction Kinetics Software*, University of Bern: Chemistry Departement (1997) http://iacrs1.unibe.ch/chemsoft/
13. R.E. Leuchtner, A.C. Harms, A.W. Castleman Jr, J. Chem. Phys. **92**, 6527 (1990)
14. K.J. Laidler, *Chemical kinetics* (HarperCollins, New York, 1987)
15. D.M. Cox, K.C. Reichmann, D.J. Trevor, A. Kaldor, J. Chem. Phys. **88**, 111 (1988)
16. H. Grönbeck, W. Andreoni, Chem. Phys. 262, 1 (2000); H. Häkkinen, U. Landman, Phys. Rev. B **62**, R2287 (2000)
17. V. Bonačić-Koutecký, private communication; H. Häkkinen, U. Landman, private communication
18. X. Wu, L. Senapati, S.N. Nayak, A. Selloni, M. Hajaligol, J. Chem. Phys. **117**, 4010 (2002)
19. H. Häkkinen, U. Landman, J. Am. Chem. Soc. **123**, 9704 (2001)
20. S. Wolf, G. Sommerer, S. Rutz, E. Schreiber, T. Leisner, L. Wöste, R.S. Berry, Phys. Rev. Lett. **74**, 4177 (1995)
21. H. Häkkinen, M. Moseler, U. Landman, Phys. Rev. Lett. **89**, 033401 (2002)